19th Australasian Fluid Mechanics Conference
Melbourne, Australia
8-11 December 2014

Two-point Correlations in Turbulent Boundary Layers and Channels up to δ^+=2000

J. A. Sillero and J. Jiménez

School of Aeronautics, U. Politécnica de Madrid, 28040 Madrid, Spain

Abstract

A new comparison of the three-dimensional two-point correlations for the streamwise (u), wall-normal (v), and spanwise (w) velocity fluctuations, is presented for turbulent boundary layers and channels reaching $\delta^+ \approx 2000$. Streamwise, spanwise and wall-normal dimensions and inclinations angles are given, with special emphasis on the behavior of the logarithmic and outer layers. The correlations are fairly different for different variables. In general, C_{uu} is inclined at shallow forward angles to the wall, which vary with the wall distance. C_{ww} is inclined at a steeper angle, but still forward, and C_{vv} is essentially vertical. The streamwise velocity component is found to be coherent over longer distances in channels than in boundary layers, especially in the direction of the flow. For weakly correlated structures, the maximum streamwise length at the outer region is $\mathcal{O}(7\delta)$ for boundary layers and $\mathcal{O}(18\delta)$ for channels. The corresponding lengths for the spanwise and wall-normal velocities are shorter, $\mathcal{O}(\delta$-$2\delta)$. Further insight into the flow is provided by correlations conditioned on the intensity of the perturbations at the reference point, or on their sign. The statistics of the new simulation are available in `http://torroja.dmt.upm.es/turbdata/blayers/`

Introduction and Methods

The purpose of this paper is to present fully three-dimensional two-point statistics of a new zero-pressure-gradient turbulent boundary layer [8] up to $Re_\theta \approx 6600$ ($\delta^+ \approx 2000$), which is compared with turbulent channels at similar maximum Reynolds number, $\delta^+ = 2003$ [2], where δ is either the boundary-layer thickness or the channel half width. Those two types of flows are used as archetypes of external and internal wall-bounded flows respectively. In our study, spatial velocity correlations are computed within fairly long domains, $\mathcal{O}(20\delta)$, to allow the fluid structures to fully decorrelate and to observe the largest scales present in the flow. Table 1 summarizes the main parameters of the direct numerical simulations used in this paper.

Case	δ^+	$(L_x, L_y, L_z)/\delta$	N_x, N_y, N_z
CH2000	2003	$8\pi, 2, 3\pi$	$6144, 633, 4608$
BL6600	980–2025	$21\pi, 3.5, 3.2\pi$	$15361, 535, 4096$

Table 1. Parameters of the numerical simulations. L_x, L_y and L_z are the box dimensions along the three axes, and N_x, N_y and N_z are the collocation grid sizes.

The paper discusses the average three-dimensional organization and structure of the flow in terms of spatial two-point correlation functions, that are computed in Fourier space for all the homogeneous directions. For instance the covariance in boundary layers is defined as

$$\widehat{R}_{\psi\phi}(x,x',y,y',k_z) = \langle \widehat{\psi}(x,y,k_z)\widehat{\phi}^*(x',y',k_z)\rangle, \qquad (1)$$

where ψ and ϕ are generic variables of zero mean, $\widehat{\psi}$ stands for Fourier transformation with respect to z, and $\langle\cdot\rangle$ is the expected value. The asterisk is complex conjugation, and k_z is the spanwise wave number. The covariance in physical space, $R_{\psi\phi}(x,x',y,y',\Delta z)$, is obtained as the inverse Fourier transform of $\widehat{R}$, where $\Delta z = z - z'$ is the distance between the two points in the spanwise direction. The autocorrelation coefficient,

$$C_{\psi\phi}(\mathbf{r},\mathbf{r}') = \mathbf{R}_{\psi\phi}(\mathbf{r},\mathbf{r}')/\sigma_\psi(\mathbf{r})\sigma_\phi(\mathbf{r}'), \qquad (2)$$

is obtained by normalizing the covariance with the product of the standard deviations at the two points involved in the measurements, denoted by $\mathbf{r}'$ for the reference point and by $\mathbf{r}$ for the moving one.

Since boundary layers are not homogeneous in the x-direction, correlations are only compiled at two reference sections, chosen so that $\delta(x')^+$=1530 and 1990. In each case, the streamwise range is $x = x' \pm 10\delta$, except for the most downstream location, where the computational box ends at $x_{end} \approx x' + 2\delta$. The correlations in the channel is computed over the whole computational box, $x = x' \pm 4\pi\delta$. In all cases, the covariances are accumulated over all the statistically independent flow field realizations of our numerical databases, $\mathcal{O}(200)$, and compiled for more than twenty different heights distributed over the inner, logarithmic, and outer regions of the flow.

Velocity Correlation Results

Figure 1 is a three-dimensional representation of C_{uu} for the boundary layer, centered in the outer region, $y'/\delta = 0.6$, and $\delta(x')^+ = 1530$. For the isosurface $C_{uu} = 0.09$, there is a positively correlated region extending about $L_x \approx 4\delta$ between its farthermost points in the streamwise direction, from 3δ upstream to δ downstream of the reference point. In the wall-normal and spanwise directions, its size is $L_y \approx \delta$ and $L_z \approx 0.5\delta$, respectively. Two negatively correlated regions flank the positive one, separated from each other by $\Delta z \approx \delta$ and with sizes that are smaller than the positive one. Both the positive and negative regions are slightly inclined with respect to the wall.

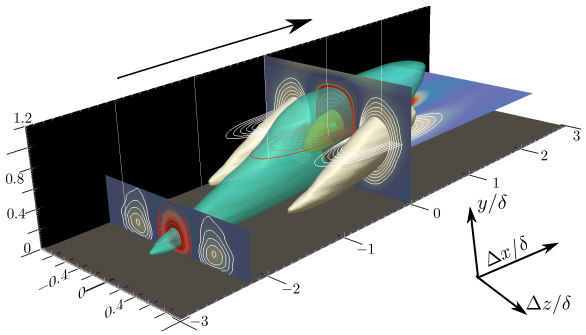

Figure 1. 3D representation of C_{uu} for BL6600 at δ^+=1530 and y'/δ=0.6. Several isosurfaces are shown at C_{uu}=−0.09 (white), +0.09 (turquoise), +0.4 (yellow) and +0.8 (blue). In the planes going through the correlation origin, the contour lines of positive and negative correlation values are colored red and white respectively, ranging from 0.09 to 1.0 and from -0.04 to -0.1. The contour lines of the zy-plane at $\Delta x/\delta$=−2.2 range from 0.03 to 0.1, and from -0.02 to -0.06.

The functional form of the correlations in those sections is not

completely arbitrary, because it follows from incompressibility that the covariance must satisfy $\sum_j \partial_j R_{ji}(\mathbf{r},\mathbf{r}') = 0$, where ∂_j is the derivative with respect to r_j, and j refers to the coordinate direction or to the corresponding velocity component. Integrating over the whole domain, and noting that the correlation vanishes at large $|\mathbf{r}-\mathbf{r}'|$, or whenever $\mathbf{r}$ is at a no-slip wall, it follows that

$$\iint R_{uu}\,\mathrm{d}z\,\mathrm{d}y = \iint R_{vv}\,\mathrm{d}x\,\mathrm{d}z = \iint R_{ww}\,\mathrm{d}x\,\mathrm{d}y = 0. \qquad (3)$$

The integrations in equation (3) are over a full plane normal to each velocity component: from $(-\infty,\infty)$ in the case of x and z; from one wall to the other in the case of y in channels; and from the wall to the potential stream in the case of y in the boundary layer. Therefore, the correlation flux over planes orthogonal to a given velocity component has to vanish, implying the coexistence of positive and negative correlation regions within each plane. This can be seen in figure 1 for the two cross-flow sections of C_{uu}. Note that equation (3) does not require the plane to pass through the origin, and that it does not apply strictly to the correlation coefficient in inhomogeneous flows, because of the spatial dependence of the standard deviations.

Two-dimensional Sections

The streamwise (xy) sections of C_{uu} centred at $y' \approx 0.8\delta$ are given in figure 2, showing that channels are significantly longer than boundary layers. This agrees qualitatively with published spectra [5], but it is important to understand that correlations and spectra are not strictly equivalent. In the first place, streamwise spatial spectra in inhomogeneous boundary layers can only be defined approximately. Secondly, a spectrum at a fixed y, or even a set of spectra at several heights, contain different information from that in a two-dimensional correlation. Consider, for example, figure 3 that shows C_{ww}. Taking as a reference the isocontour $C_{ww} = 0.05$, any analysis involving only $y = 0.8\delta$ would suggest correlations lengths of the order of $L_x \approx 0.7\delta$, while the 2D correlation shows that the structure is longer. The maximum streamwise distance $L_x^m \approx 2.5\delta$, is between points at different heights, because the structure is relatively thin but long and inclined forwards. The effect is also present in C_{uu} as showed in figure 2, although less marked.

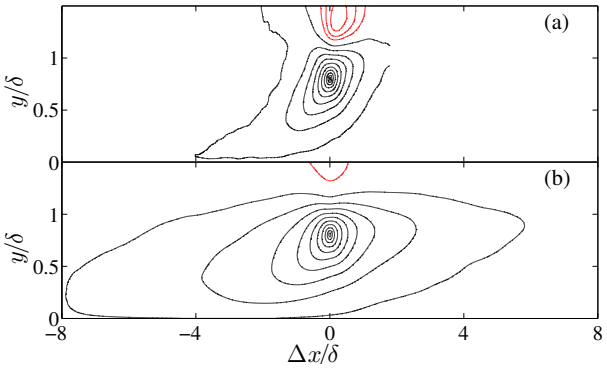

Figure 2. Streamwise (xy) sections of C_{uu} at y'/δ=0.8. (a) BL6600 at $\delta^+ \approx 2000$. (b) CH2000. Positive contours (black) are (0.05:0.1:...), and negative ones (red) are (-0.05:-0.05:...). Flow is from left to right.

Using the same correlation isocontour (0.05), C_{uu} extends for $L_x^m \approx 6\delta$ in boundary layers, and for $L_x^m \approx 15\delta$ in channels. In the y-direction, C_{uu} spans the whole flow thickness, from very close to the wall to either the potential stream or to beyond the channel centerline, whereas C_{ww} is flatter. Both correlations are inclined forwards, presumably as a consequence of the shearing by the mean velocity profile. Very long features have been reported in the logarithmic and outer layers of all wall-bounded flows, variously referred to as "largest", "very large", or "global". They are known to be correlated across the full boundary layer thickness [1], and to penetrate the sublayer. The streamwise lengths given for C_{uu} in boundary layers are typically $\mathcal{O}(4\delta\text{-}5\delta)$, independent of the Reynolds number [3], while those in channels and pipes tend to be closer to $\mathcal{O}(9\delta\text{-}20\delta)$ [6]. Those numbers are in general agreement with figure 2. In all the cases C_{uu} is longer than C_{ww}, as can be seen by comparison of figure 2 with figure 3, whereas C_{ww} exhibits similar correlation lengths in both flows, $\mathcal{O}(2\delta)$.

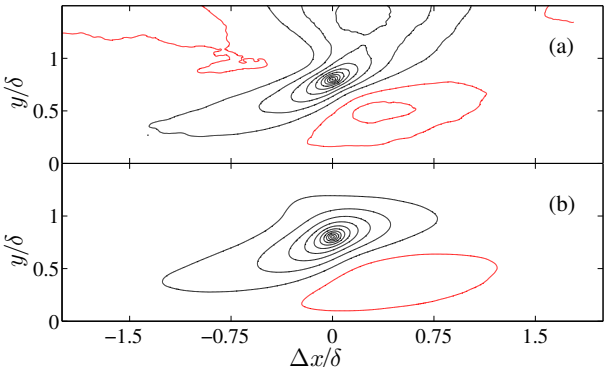

Figure 3. As in figure 2, for C_{ww}.

It follows from equation (2) that $C(y,y',x,x')$=$C(y',y,x',x)$, so that, if the correlations centered far from the wall extend into the inner layer, those centered near the wall must extend into the outer layers with comparable streamwise dimensions. For example, neglecting the streamwise inhomogeneity of the boundary layer, the correlation along y=0.1δ in figure 2 would correspond (not shown) to the x-reflection of the correlation along y=0.8δ when centered at y'=0.1δ, and their streamwise dimensions must be identical. That agrees with the notion that energy from the larger outer structures reaches the near-wall layer [2], and in essence, it reflects that the correlations in that range of wall distances represent, at least in part, different aspects of the same large-scale structure extending from the top of the buffer layer to the outer edge of the flow.

In contrast to the streamwise sections, figure 4 shows that the spatial organization of the correlations in the cross-flow (zy) plane is qualitatively similar for boundary layers and channels, which are shown side-by-side along the spanwise direction, because of symmetry.

The streaky pattern of the u-structures is revealed in figures 4(a,b), with alternating low- and high-momentum regions separated by distances of $\mathcal{O}(\delta)$. As in the case of the streamwise sections, C_{uu} is also the correlation in which channels differ more from boundary layers, with the longer streaks of the channels associated to somewhat wider and taller cross-sections. It is interesting that, although the streak separation gets wider with increasing wall distance, it grows more slowly than proportionally to y'. It can be shown that the streak spacing scales in outer units, as inferred by comparing these correlations with lower Reynolds numbers cases [9].

The sections of C_{vv} in figures 4(c,d) are narrower than those of C_{uu} near the wall, although the dimensions of the two variables are much closer to each other in the outer layer. The scale of C_{vv} hence varies strongly with y', as shown repeatedly by previously published spectral measurements. The cross-sections of C_{ww} are shown in figures 4(e,f). Their positive lobes are thin-

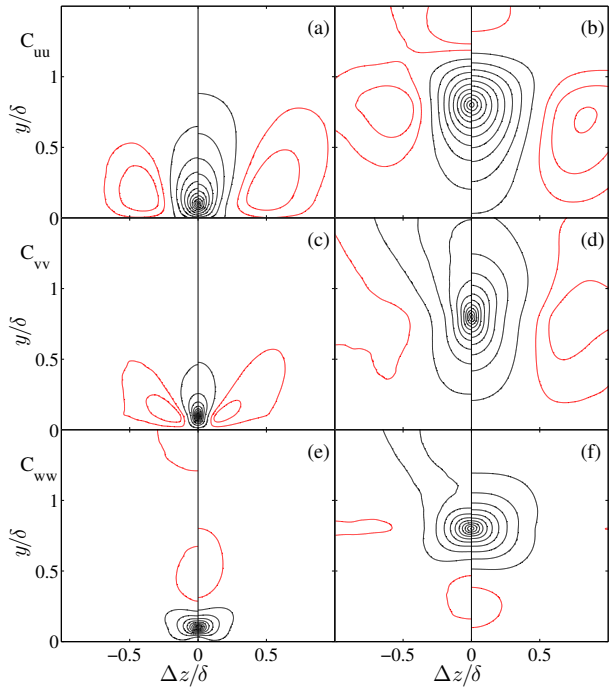

Figure 4. Cross-flow (zy) sections of the correlations at: (a,c,e) y'/δ=0.1, and (b,d,f) y'/δ=0.8. (a–b) C_{uu}. (c–d) C_{vv}. (e–f) C_{ww}. For each panel, the left side is BL6600 at $\delta^+ \approx 2000$ and the right side CH2000. The positive contours (black) are (0.05:0.1:...). The negative contours (red) are (-0.05:-0.05:...), except for (c–d), whose values are (-0.01:-0.02:...).

ner in the wall-normal direction than either C_{uu} or C_{vv}, but the full correlation, including positive and negative regions, spans a large fraction of the flow thickness and its wall-parallel dimensions vary relatively little with y'. As a consequence, the positive contours of C_{ww} are relatively flat near the wall, and more square away from it. It follows from the continuity condition that the integral of C_{ww} should vanish over the xy-plane, and figure 3 shows that the cancellation takes the form of alternating relatively thin layers stacked in the y-direction. The intersection of these inclined layers with the cross plane appears in figures 4(e,f) as negative lobes above or below the primary positive contours. The combination of C_{vv} and C_{ww} in the zy-sections suggests a quasi-streamwise roller with dimensions of $\mathcal{O}(\delta)$, which the streamwise sections in figure 3 show to be inclined with respect to the wall. As in the case of the cross-sections of the u-streaks, the agreement at different Reynolds numbers (not shown) suggests that the roller dimensions scale in outer units [9].

Inspection of the (xy) sections of the correlations shows that those are inclined to the wall, with an inclination angle that depends of the chosen isocontour. Consider a correlation isocontour for a given variable at a given y'. Its (xy) section can be approximated by an ellipse having the same second-order tensor of inertia. The inclination α is defined as the angle between the major semiaxis of that ellipse and the x axis, and a characteristic inclination angle is defined as the maximum angle found at a given height. This is shown in figure 5. The angles for each velocity component are remarkably uniform across most of the flow, although different from each other. They agree much better between boundary-layers and channels than other measures because the maximum inclinations correspond to relatively small structures controlled by local, rather than global, processes. Experimental and numerical data is included in the

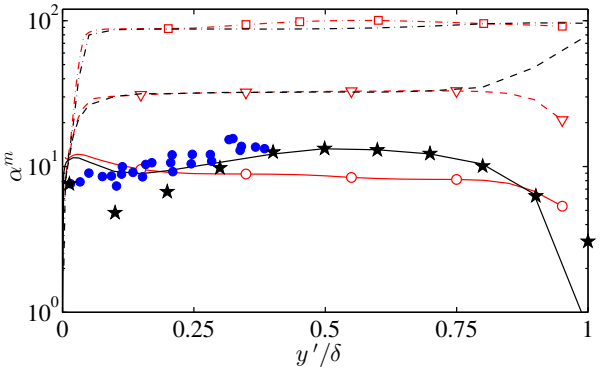

Figure 5. Maximum inclination angle as a function of y'/δ. ———, α_u; — · —, α_v; - - - -, α_w. Lines without symbols are BL6600 at $\delta^+ \approx 2000$, and those with empty symbols CH2000. ⋆ is a numerical compressible boundary layer [7], and ● are experimental smooth and rough boundary layers [11].

figure, and agree with our measurements. These angles should be interpreted to mean that u is strongest when the structures are aligned to the streamwise direction, v is strongest when they are normal to the wall, and w is intermediate between the two [4], because correlations are statistical measures that weight the geometry of a given velocity field with its squared intensity. Any characteristic number extracted from the correlation of some variable most probably represents its geometry when the variable is strongest.

Conditional Correlations

The correlation $C_{\psi\phi}$ describes the mean value of $\psi(\mathbf{r})$ conditioned to that of $\phi(\mathbf{r}')$ but, because it is an average, it retains no information about the functional relation between the two variables. If that relation is linear, Linear Stochastic Estimation (LSE) [10] provides a best estimate for $\psi(\mathbf{r})$ in terms of $\phi(\mathbf{r}')$, but nonlinear relations require higher-order estimates, or conditional statistics. Define the positive conditional correlation,

$$C^{\oplus}_{\psi\phi}(\mathbf{r},\mathbf{r}')|_{\xi} = \frac{\langle \psi(\mathbf{r})\cdot\phi(\mathbf{r}')\rangle|_{\xi(\mathbf{r}')>\mu}}{\sigma_{\psi}(\mathbf{r})\cdot\sigma_{\phi}(\mathbf{r}')|_{\xi(\mathbf{r}')>\mu}} \qquad (4)$$

where the three variables involved are not necessarily the same, and the condition is that $\xi(\mathbf{r}')$ has to be stronger than a given threshold μ, typically chosen as a fraction of $\sigma_{\xi}(y')$.

A consequence of the symmetry of the problem in the spanwise direction is that correlations would be symmetric in z even if the underlying structures were not. Consider C_{ww} conditioned on the positive sign of w (μ=0), $C^{\oplus}_{ww}|_w$, presented in figure 6. In both flows, the conditional correlations are aligned to the 45° diagonal, most clearly so for the boundary layer. By symmetry, $C^{\ominus}_{ww}|_w$ is aligned to the opposite diagonal, and is not shown. The effect is stronger far from the wall. The shaded contours that correspond to y'/δ=0.1 are actually slightly inclined in the opposite direction to those away from the wall. Since we saw in figure 4 that w changes sign near the wall, this negative inclination is probably due to that counterflow. Unfortunately, we cannot offer at the moment an explanation for this structure.

That w is also able to distort u is tested by $C^{\oplus}_{uu}|_w$ in figure 7. The skew is now only $\sim 7^{\circ}$, and probably corresponds to the meandering discussed in Hutchins and Marusic [3]. It can only be clearly seen when conditioning by relatively strong velocities, μ=1.5σ_w, but it suggests that the meandering of u is a consequence of the more obvious diagonal organization of w.

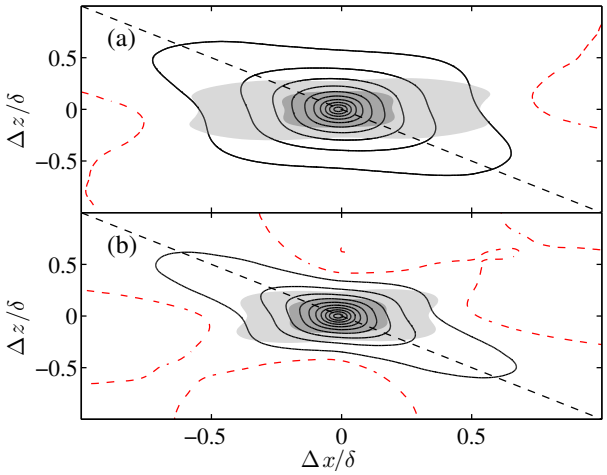

Figure 6. Wall-parallel sections of $C^{\oplus}_{ww}|_w$ at y'/δ=0.1 (shaded) and y'/δ=0.8 (lines) conditioned to $w > 0$. (a) CH2000. (b) BL6600 at $\delta^+ \approx 1530$. Positive contours (black solid lines) are $(0.05 : 0.1 : \ldots)$. Negative contours (red dashed lines) are $-(0.01 : 0.05 : \ldots)$. The shaded contours are 0.1,0.3. The dashed diagonal is inclined at 45° to the mean velocity.

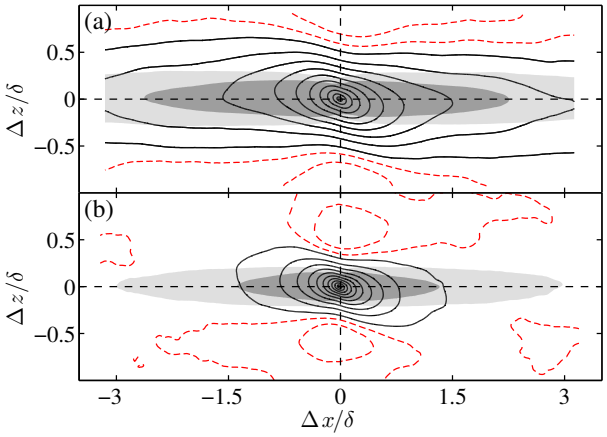

Figure 7. Wall-parallel sections of $C^{\oplus}_{uu}|_w$ conditioned to $w > 1.5\sigma_w$. (a) CH2000. (b) BL6600 at $\delta^+ \approx 1530$. Colors and lines as in figure 6.

Conclusions

Fully 3D two-point statistics of a new zero-pressure-gradient turbulent boundary layer up to $Re_\theta \approx 6600$ ($\delta^+ \approx 2000$) have been presented and compared with turbulent channels at similar Reynolds numbers. We considered very large domains $\mathcal{O}(20\delta)$ to observe the largest scales present in the flow and to educe the average spatial structure of the velocity fluctuations. We have shown that C_{uu} is coherent over longer distances in channels than in boundary layers, especially in the direction of the flow. Along that direction, the maximum length of the weakly correlated structures is $\mathcal{O}(18\delta)$ in channels and $\mathcal{O}(7\delta)$ in boundary layers. We argue that those correlation lengths do not change significantly from the near-wall to the outer region because they essentially reflect different aspects of a common large-scale structure, implying that the energy from the larger outer structures reaches the neighborhood of the wall. Along the spanwise direction the three velocity components present similar widths, $\mathcal{O}(\delta)$. The correlations are shown to be inclined to the wall with different maximum angles that are remarkably uniform across most of the flow and differ little between channels and boundary layers. The spatial organization of w was shown to consist in the superposition of two diagonal orientations. Conditioning the wall-parallel sections of C_{ww} on the sign of w results in a correlation that is aligned at $\pm 45^o$ to the mean flow in the outer layer, although not near the wall. Similarly conditioning C_{uu} on intense events of w results in correlations inclined at $\pm 7^o$ only in the outer region. This suggests that the meandering of u is a consequence of the spatial organization of w, although further research is needed to clarify the mechanism that leads to that organization.

Acknowledgements

This research was funded in part by the European Research Council under grant ERC-2010.AdG-20100224. It used the computational resources of the Argonne Leadership Computing Facility at Argonne National Laboratory, which is supported by the Office of Science of the U.S. Department of Energy under contract DE-AC02-06CH11357. J.A. Sillero was supported in part by an FPU fellowship from the U. Politécnica de Madrid.

References

[1] Bullock, K. J., Cooper, R. E. and Abernathy, F. H., Structural similarity in radial correlations and spectra of longitudinal velocity fluctuations in pipe flow, *J. Fluid Mech.*, **88**, 1978, 585–608.

[2] Hoyas, S. and Jiménez, J., Scaling of the velocity fluctuations in turbulent channels up to $Re_\tau = 2003$, *Phys. Fluids*, **18**, 2006, 011702.

[3] Hutchins, N. and Marusic, I., Evidence of very long meandering features in the logarithmic region of turbulent boundary layers, *J. Fluid Mech.*, **579**, 2007, 467–477.

[4] Jiménez, J., How linear is wall-bounded turbulence?, *Phys. Fluids*, **25**, 2013, 110814.

[5] Jiménez, J., Hoyas, S., Simens, M. P. and Mizuno, Y., Turbulent boundary layers and channels at moderate Reynolds numbers, *J. Fluid Mech.*, **657**, 2010, 335–360.

[6] Lozano-Durán, A. and Jiménez, J., Effect of the computational domain on direct simulations of turbulent channels up to Re_τ=4200, *Phys. Fluids*, **26**, 2014, –.

[7] Pirozzoli, S. and Bernardini, M., Turbulence in supersonic boundary layers at moderate Reynolds number, *J. Fluid Mech.*, **688**, 2011, 120–168.

[8] Sillero, J. A., Jiménez, J. and Moser, R. D., One-point statistics for turbulent wall-bounded flows at Reynolds numbers up to $\delta^+ \approx 2000$, *Phys. Fluids*, **25**, 2013, 105102.

[9] Sillero, J. A., Jiménez, J. and Moser, R. D., Two-point statistics for turbulent boundary layers and channels at Reynolds numbers up to $\delta^+ \approx 2000$, *Phys. Fluids*, (Submitted).

[10] Tomkins, C. D. and Adrian, R. J., Spanwise structure and scale growth in turbulent boundary layers, *J. Fluid Mech.*, **490**, 2003, 37–74.

[11] Wu, Y. and Christensen, K. T., Spatial structure of a turbulent boundary layer with irregular surface roughness, *J. Fluid Mech.*, **655**, 2010, 380–418.